Journal of CO2 Utilization 88 (2024) 102931

Contents lists available at ScienceDirect

Journal of CO2 Utilization

journal homepage: www.elsevier.com/locate/jcou

Carbon dioxide valorisation with partial oxidation of methane in a water cooled DBD plasma

Nicola Lisi , Umberto Pasqual Laverdura *

ENEA CR Casaccia, Via Anguillarese 301, Roma 00123, Italy

ARTICLE INFO

Keywords:
Dielectric barrrier discharge
Low temperature plasma
CO2 dissociation
Hydrogen
Greenhouse

ABSTRACT

The valorisation of carbon dioxide in chemical plasmas implies as a principal reaction step its energy efficient dissociation into carbon monoxide. For hydrogen production, the reaction carbon monoxide with water (WGS) may lead to the generation of green hydrogen and reusable carbon dioxide. Beyond hydrogen, most valorisation processes require the removal of O_2 to avoid its recombination with CO on any downstream hot catalytic surface. Moreover, if the oxygen scavenging is performed directly inside the plasma volume, it can also shift the dissociation equilibrium that is responsible for the well-known trade-off between energy efficiency and conversion, thus improving efficiency when larger specific energy densities are applied. In this paper we first report on the plasma dissociation of pure CO_2 in a water cooled, high power(<2 kW), Dielectric Barrier Discharge with high gas flow regime (<3600sccm), and then we explore the synergistic oxygen removal by the partial oxidation of methane for syngas production. The presence of CH_4, even in small amounts, removes oxygen from the outstream and from the discharge region, as confirmed by mass and optical emission spectroscopies, and enhances the process in two ways: it allows to feed the system with gas having a low CH_4 to CO_2 ratio (0.1–0.3) instead of pure CO_2, where landfill and waste gases are undesired climate altering emissions with a similar composition that currently require flaring; it will allow to use directly the reactor outstream into a WGS reactor, or any other CO valorisation process without the necessity to remove downstream O_2.

1. Introduction

The Dielectric Barrier Discharge (DBD) technology is currently among the best suited plasma generation technologies [1] for the reproducible, stable, and clean plasma processing: the absence of direct currents and the electrode-less discharge effectively inhibit thermal runaways and arching, at a time of history that benefits of the availability of high power and frequency switching components in silicon and other materials (Si, SiC, GaAs, GaN), for high frequency, high power electric driver design.

The plasmo-chemical generation of hydrogen [2,3] is a concept proposed in the final quarter of the last century, based on a closed loop CO_2 cycle: its dissociation in CO and O_2, the separation of CO, its reaction with H_2O to produce H_2 and CO_2, the separation of H_2 and the reuse of CO_2.

This method of producing H_2, if made sufficiently energy efficient, implements a power to gas scheme with some interesting points: namely the absence of components based on critical, toxic or precious metals, the absence of catalysts in the main dissociation reaction step, and the fast on-off capabilities of high power discharge plasmas that can digest low value, fast electric energy transient excesses from renewable sources and production excesses that drive to negative energy prices.

While such “benchmark” scheme for the plasmo-chemical production of H_2 uses CO_2 in an ideal closed loop, CO and H_2 can also be applied as reaction intermediates in any number of other power-to-fuel and power-to-gas carbon neutral [4–6] or even negative, schemes. Here on the feed stream side, a pure CO_2 feed is necessary if one wants to avoid expensive noble gas dilution [7], however CO_2 is readily available as a largely undesired climate altering emission either as a combustion flue gas (CO_2/N_2=0.1–0,2) [8] or as industrial low grade waste gas or landfill gas (CO_2/CH_4>1), or as high grade biogas from organic waste (CO_2/CH_4<0.3) [9].

The energy efficiency of plasma dissociation of high purity CO_2 in microwave excited plasmas has been reported to reach large values, up to 90 % in microwave (MW) excited supersonic flows [10], but always with a trade-off between energy efficiency and conversion rate: large efficiency could be achieved only at low conversion rates [3,11,12].

All subsequent studies so far confirmed some version of this trade-off

* Corresponding author.
E-mail addresses: nicola.lisi@enea.it (N. Lisi), umberto.pasqual@enea.it (U. Pasqual Laverdura).

https://doi.org/10.1016/j.jcou.2024.102931
Received 2 July 2024; Received in revised form 3 September 2024; Accepted 13 September 2024
Available online 19 September 2024

between energy efficiency and conversion. Energy efficient operations imply low conversions, that brings up the importance of gas separation for any practical application of the scheme. Beside the energy efficiency of the dissociation process itself, mainly limited by the difficulties in achieving ideal plasma parameters for the vibrational dissociation by the impact of a large population of low energy (≈1 eV) electrons [3,13], also the energy efficient separation of the different gas phases involved in the process must be achieved, both on the input (pure CO_2) and output side (no O_2) of the process.

In recent years the concept for the removal of oxygen from the plasma regions by inserting oxygen selective solid state membrane barriers has been developed [14], but the permeate flow remains short of the required oxygen flow, while there are severe membrane sealing, scaling, and lifetime issues [15].

The possibility to implement the dry reforming of CH_4 inside a plasma reactor has been widely investigated [16,17], both with and without catalysts inside the reactor. While most of the studies focused on the enhancement of the typical reforming process (CH_4/CO_2=2/1), by approaching the conversion of methane into hydrogen with a "plasma hammer", we instead investigated the enhancement of CO_2 dissociation with the help some methane when CO_2/CH_4>3.

Interestingly this reaction, in methane poor conditions (CO_2/CH_4=4) was investigated in a high power (500 W) DBD reactor by Kogelshatz group [17] aiming at the formation of higher hydrocarbons.

Instead, in processes aiming at the valorisation of CO_2, and specifically for methanation, it is difficult to imagine how the presence a plasma that splits CO_2 into oxygen may benefit the process, since CH_4 and H_2 readily react and "burn" with it into water under plasma activation, scavenging hydrogen and plasma energy, and impairing the overall conversion process.

The reforming of even CH_4, CO_2 mixtures (CH_4/CO_2=1/1) at 15slm each in a high power, atmospheric pressure microwave plasma torch [18] did result into the dissociations of most of the methane and almost 70 % of the CO_2 to syngas at 6 kW plasma power. Similar studies have been conducted in DBD reactors at lower power and smaller gas flows studying methane rich [19], with a few percent methane conversion, and methane poor mixtures [20], where larger methane conversions were observed, aiming at the production of hydrogen from biogas.

In this paper instead we report the on the effects of adding small amounts of methane that undergo partial oxidation, up to 1/3 of the main CO_2 flow, to increase the conversion into CO and add H_2 to the outstream and evaluate the possible benefits for the overall CO_2 dissociation process: a low grade gaseous input stream, higher conversion and energy efficiency, and the removal of oxygen from the outstream, while we also extended the study of the process pressure up to 3 bar.

With respect to the microwave plasma torch [18] where the gas temperature was spectroscopically measured to reach nearly 6500°C, we also expect to maintain a lower gas temperature in the water cooled DBD discharge [12].

The combination of CO_2 and CH_4 to produce syngas was also investigated in a multi electrode DBD discharge [21] in principle capable to excite large gas flows, applying up to 120sccm of CH_4 and CO_2 and 90 W power.

Summarising, the main objective of the present study is to find out if by the addiction of small quantities of CH_4 to a main CO_2 flow that undergoes partial oxidation, it is possible to increase its conversion in CO, produce some H_2, and to get rid of the O_2 that impairs the downstream application flow from the flow as condensed water.

By applying the high-power water cooled DBD reactor that operates at low temperature and high pressure we expect to drive the reaction towards the condensation of water with no mole increase, with respect to syngas production, that doubles the moles. In this vision, in the "limit" case of full CO_2 dissociation into CO, the quantity of methane in the inlet should be limited to one fourth of the total to aim at their complete reaction into monoxide and water:

$$3CO_2 + CH_4 \Rightarrow^{plasma} 4CO + 2H_2O \quad (1)$$

The main idea behind this reaction scheme and stoichiometry is the partial oxidation of CH_4 [22,23] by the oxygen available from the dissociation of CO_2, imagining that the overall process might occur in two steps, the first being the plasma dissociation itself:

$$CO_2 \Rightarrow^{plasma} CO + \frac{1}{2}O_2 \quad (2)$$

That may also occur into atomic oxygen without the formation of O_2, unlike (2).

The second reaction is the reaction of methane with oxygen, involving the CH_4 molecule or plasma generated atoms and radical fragments that become available in the plasma. This reaction is simplified here (3) and (4) as a partial oxidation, since also CH_4 is dissociated in the plasma and in this path to pyrolysis [3] many intermediates will form and will be available to react with oxygen [21,22].

$$CH_4 + \frac{1}{2}O_2 \Rightarrow^{plasma} CO + 2H_2 \quad (3)$$

$$CH_4 + O_2 \Rightarrow^{plasma} CO + H_2 + H_2O \quad (4)$$

It is worthy to notice that following the plasma dissociation of molecules, the produced O and H atoms do not need to recombine into their respective molecules for the set of reactions to proceed into the desired produces: H_2O, CO and H_2.

Overall, the different possible atomic, radical, and atomic reaction channels contribute towards reaction (1).

Given that the reactor discharge is efficiently water cooled and can operate at atmospheric pressure and above, up to 3 bar in the current study, the aim of the present work is to investigate the hypothesis that the efficient subtraction of oxygen and its condensation into liquid water may drive the CO_2 dissociation reaction towards higher conversions rates so that the reactions (2) and (3,4) may act synergistically.

It is also interesting to speculate whether the presence of a positive enthalpy driving the reactions (3,4) (a kind of flame plasma [22]) could also be beneficial towards plasma ignition, and for driving the discharge plasma into a better regime (lower electric field and higher electron density) for the CO_2 dissociation process itself.

It should be added that due to the absence of oxygen may also drive some of the CO to disproportionate into solid carbon if appropriate conditions are sought of and engineered for, such a hot downstream catalytic or carbon bed [24] suggesting strategies beyond hydrogen generation by WGS [25] for CO_2 valorisation [26].

The two main channels for the plasma dissociation of CO_2 are the energy efficient vibrational excitation by successive low energy (≈1 eV) electron collision into auto-dissociative states and the less efficient direct dissociation by electron impacts [3]. On the downside, the presence of some amount of hydrogen (and water) in the plasma reaction (1) will probably have a negative effect on the dissociation of CO_2, an effect that was well known, and sought for, in CO_2 laser science [27,28]. The proposed a mechanism was based on the quenching of the vibrational (auto-dissociative) excitation of CO_2 by collisions with light He and H_2 [29], while others had proposed the reaction of CO with OH radicals back into CO_2 [22], and even attributed the effect to the oxygen sequestration in the oxidation of the electrodes [30].

There are two main reasons for considering an oversimplified kinetics. The first is that at the core of the practical aim of the process presented here is (or eventually it will be) the energy efficient vibrational dissociation of CO_2 by a large population of low energy electrons and the synergistic sequestration of the oxygen that is liberated, by the partial oxidation of methane to produce an oxygen free CO and H_2 stream.

If the first part of the process (i.e. the efficient vibrational dissociation of CO_2) will be eventually achieved in DBD reactors, then we expect that the second part (i.e. the reaction of oxygen with methane) will occur

spontaneously and fast.

All the other plasma reactions, the generation excited species, the direct electron impact dissociation of molecules and radicals, the plasma pyrolysis of methane, the ionization of atoms, radicals and molecules are all "unwanted" processes that are deemed to reduce the energy efficiency, that is critical for the feasibility of the greater goal of reducing overall greenhouse gas footprint.

In conclusion the reason for considering a more complex kinetics has more to do with the DBD drawbacks and failure in pairing microwave results [31] (due to the excessively high reduced electric field that activates too many reaction channels), than to the achievement of useful goals for an energy efficient process.

Also, the failure of the DBD systems to maintain the energy efficiency when scaling both gas flow and power [12] indicates that discharge filamentation [32] and inhomogeneous discharge filling and time structure are probably to blame where also thermal effect play greater than a more complex kinetics. The prominence of discharge inhomogeneities that leads to the formation of streamers and arching with respect to kinetics [33] was already recognized for chemical plasma lasers.

In the current paper, first we extent the range of the explored parameters of our previous study [12] by presenting the results on the dissociation of pure CO_2 up to high power, 2 kW, high flow, up to 3600sccm, and small gap, d≈1 mm, applying water cooled inner electrodes made of different metals with different thermal conductivity and surface chemistry: stainless steel AISI316 (SS), copper and aluminium. We want to investigate if a lower thermal conductivity and better surface passivation for steel, a higher thermal conductivity and the possibility of a different surface chemistry for aluminium and copper play a role.

Then we introduce the effects of adding different amounts of methane with and overall flow of 1000sccm (up to $1CH_4+4CO_2$) and 360sccm (up to $1CH_4+3.5CO_2$) using the same water cooled electrodes. In one experiment involving the SS electrode we also suppressed the inner electrode cooling, letting it reach a surface temperature >300°C in order explore the effect of temperature on the process. In the experiments with methane, a small Ar flow was added for calibrating the total downstream flow. In selected conditions we also extended the investigation up to 2 and 3 Bar absolute pressure.

In Fig. 1 we report the power required for the dissociation of two of the mixtures explored in the present work, namely the more methane rich conditions at the two flows. The power was simply calculated based on the bond energies of chemical species in reaction (2) and (4), on the hypothesis of the formation of highest bonded species first. Although this is a crude approximation, it shows how the presence of methane progressively lowers the reaction power. These values of power can be applied in principle to calculate the correct relation between conversion and energy efficiency of the process, if one wants to consider the energy given into the system by methane, which is then considered a high value resource.

In the current study we have been considering these low amounts of methane as an undesired waste gas, and then we have calculated the energy efficiency only based on the dissociation enthalpy of pure CO_2.

In all the experiments, the chemical environment typical of a methane-poor dry reforming leads to the formation of hydrogen and some quantity of higher hydrocarbons [17]. The formation of hydrocarbons was also monitored by mass spectroscopy by performing complete mass scans up to mass 80 at selected, high plasma power conditions. In the experiments reported here they were observed in small quantities, especially when applying the more methane rich, higher plasma power and hotter electrodes. However, although an interesting phenomenon worthy of further investigation, we did not observe these (C_nH_m) in amounts that altered the main energetics of the process. This is especially true at low reactor temperature and in the absence of a catalyst, where the main components of the outstream are CO_2, CH_4, unreacted or recombined, CO, H_2 and H_2O, the reaction products, where O_2 was always effectively removed from the stream by the presence of any inlet amount of CH_4.

2. Experimental

The experimental set-up is like that described in a previous work [34] and is schematized in Fig. 2. It consists in a quartz tube (40 mm OD, 36 mm ID) single barrier DBD system with outer water cooling and an inner metal electrode (34 mm OD) that constricts the gas flow into a ≈1 mm discharge gap, for a discharge volume of 13.2 cm^3 in the region at the reactor centre. The inner electrode is supported vertically on a tight-fitting water-cooled copper tube by means of steel and PTFE spacers, visible in figure S2. The outer electrode consists of a steel grid close-fitted to the outer quartz reactor wall that is polarized with a high voltage, variable frequency HF AC power supply (100–500 kHz), that must be tuned to the parasitic capacitance "LC" frequency to achieve plasma ignition. The outer electrode is immersed in water, improving the coupling to the quartz barrier, favouring its cooling, inhibiting ozone formation and finally with little loss towards the 400kω electrical resistance (DC measured) to the ground of the water laboratory tubes.

Gases are fed via digitally controlled mass flow controllers (MKS 179). A vacuum membrane pump can either serve to operate below atmospheric or to evacuate the system, but mainly helped to remove water after the experiments in the current set of experiments. In figure S1b) we show the inner electrodes and their cooled copper support.

The reaction products were measured by mass spectrometry (Hyden Analytical HPR-20 R&D) of the gas downstream of the reactor, by following the time evolution of selected fragments, while electrical measurements allowed to measure the plasma power, and optical emission spectroscopy (OES, Ocean HDX-XR with quartz fibre and

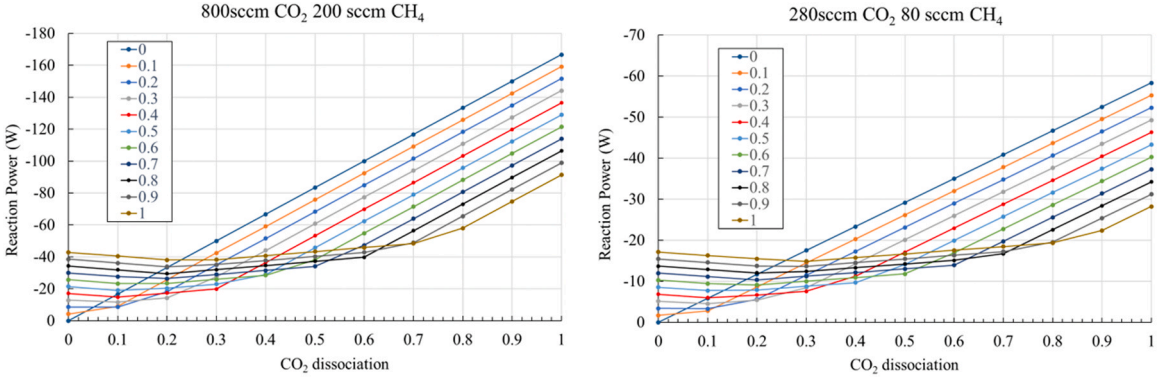

Fig. 1. The power required to drive the reaction of CO_2 and CH_4, respectively 280 and 80 sccm on the left, 800 and 200 sccm on the right, calculated for various dissociation values of CO_2 and CH_4 (values in the legend and x axis).

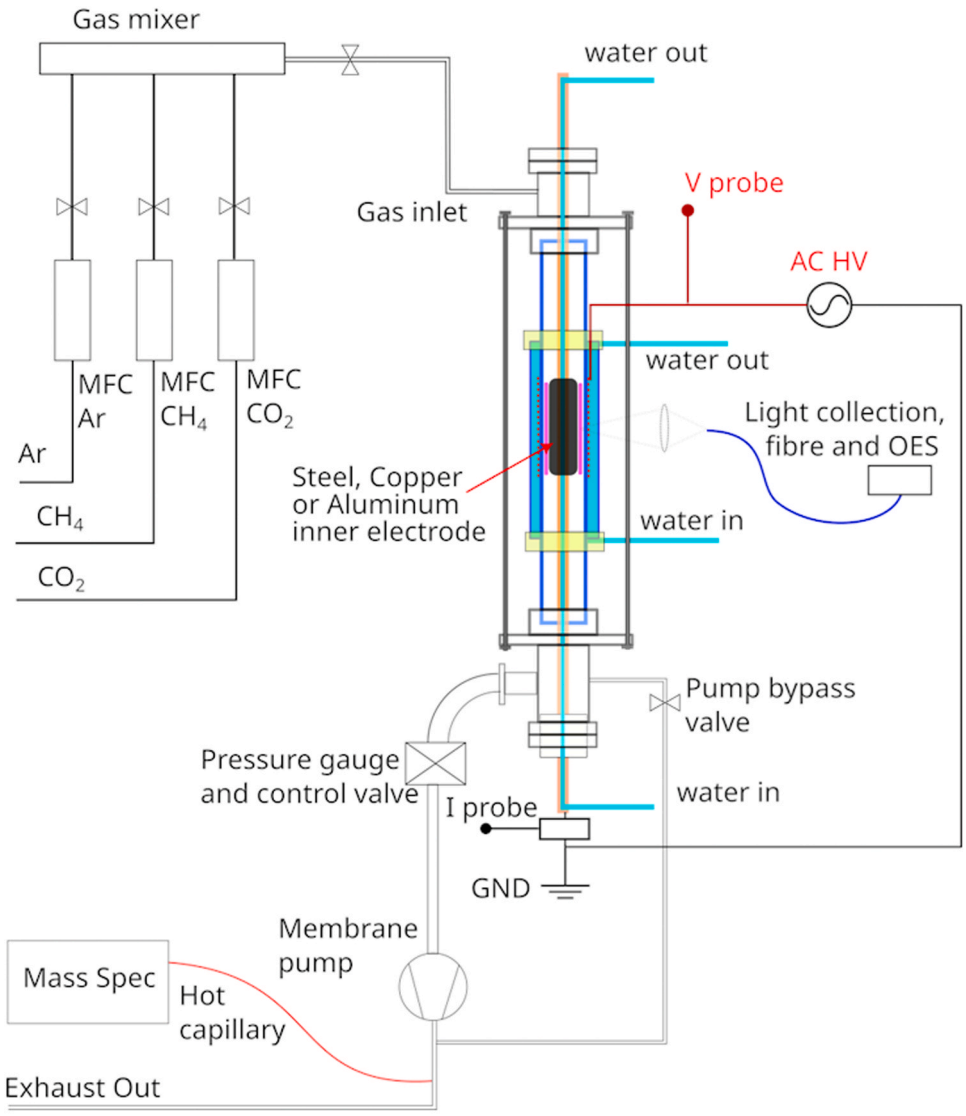

Fig. 2. Scheme of the experimental set-up, comprehensive of gas feed and diagnostics.

collection lens)) over the UV-Vis-NIR spectra allowed qualitative assessments on the process, mainly to assess the O_2 removal.

The plasma power is measured by measuring the plasma voltage and current with an oscilloscope (Tektronix TDS 200 and MSO44). The plasma voltage is measured by a high voltage high frequency probe (Tektronix P6015A) and the current by a probe connecting the inner electrode to the system ground. In this study we applied two different probes and methods for the current measurement. Initial measurements were performed with a 1 O*hm* resistive shunt and by a point-to-point product [34], later a 1.4nF capacitor was applied instead and the integration [35] of the traces was performed both on the oscilloscope or off-line. The two methods were cross checked for consistency with excellent agreement, especially when large waveform records are applied. In figure S2a) we report typical oscilloscope probe traces (and fits) applied to measure power in one of the conditions of the current study, and the relative elliptical QV Lissajous plot in figure S2b)

The power absorbed by the power supply that excited the plasma was also measured by taking the product of the RMS AC input current and voltage by means of commercial current meters (FLUKE 117 the AC voltage, FLUKE 325 the AC current).

In the current study we applied three different electrodes, as seen in figures S1a) and b), made of aluminium, stainless steel and copper. The three different materials were applied for evaluating different surface temperatures and different surface chemistry including some catalytic effect: steel has reduced thermal conductivity with respect to copper, while we expect better passivation for aluminium and steel with respect to copper. As seen in figure S1c) a simple radial heat transfer calculation shows that the steel electrode surface can reach 100°C and more despite water cooling.

In one set of experiments with SS electrode we suppressed the inner water cooling in the electrode support, inserting a thermocouple and measuring the temperature from the inner side of the copper electrode support, expecting the electrode surface to be consequently higher than that measured by the thermocouple of the values of figure S1c).(Table 1)

For each experimental condition, summarized in Tale 1 and Table 2,

Table 1
Experimental conditions for the dissociation of pure CO_2. In the last column is the specific energy input or SEI.

Pressure (bar)	CO2 (sccm)	Electrode	Power (W)	SEI (kJ/mol)
1	225	SS, Al, Cu	200–1500	1200–9000
1	450	SS, Al, Cu	200–1500	600–4500
1	900	SS, Al, Cu	200–1500	300–2250
1	1800	SS, Al, Cu	200–1500	150–1125
1	3600	SS, Al, Cu	200–1500	75–560
2	3600	SS	200–1500	75–560

Table 2
Experimental conditions for the reaction of CO_2 and CH_4.

Pressure (Bar)	CO2 (sccm)	CH4 (sccm)	Flow (sccm)	Electrode	Power (W)	SEI (kJ/mol)
1	1000	0	1000	SS, Al, SS Hot	200–1500	270–2000
1	975	25	1000	SS	200–1500	270–2000
1	950	50	1000	SS	200–1500	270–2000
1	900	100	1000	SS	200–1500	270–2000
1	800	200	1000	SS	200–1500	270–2000
1	360	0	360	SS, Al, SS Hot	200–1500	750–5600
1	330	30	360	SS, Al, SS Hot	200–1500	750–5600
1	280	80	360	SS, Al, SS Hot	200–1500	750–5600
2	280	80	360	SS, Al	200–1500	750–5600
3	280	80	360	SS, Al	200–1500	750–5600

where different electrodes, pressure, gas composition, and total flow were changed, the plasma power was varied and measured to build power conversion curves.(Fig. 3)

3. Experimental results

3.1. CO_2 dissociation at high flow and power

In Table 1 we summarize the applied conditions and in Fig. 4 the results of the dissociation of pure CO_2 with the three different electrodes, for flows larger than previously reported by our group [34].

The results are overall similar for the three electrodes, with moderately better performances for the steel electrode (3a and 3b), apparently the lower heat conduction and increased surface temperature does not impair the dissociation by increasing the recombination of CO and O_2 into CO_2, on the contrary both conversion and efficiency are improved. The curves for Aluminium and Copper are respectively in figure S3, both as function of power and SEI(kJ/Mol), and figure S4. Overall, the conversion decreased when the CO_2 flow is increasing, linked to the progressively shorter plasma gap residence time, that ranges from 1.6 s at 500sccm to 0.2 s at 4000sccm. At the same time the energy efficiency increases with the flow, while it decreases with the applied plasma power by the well-known trade-off law.

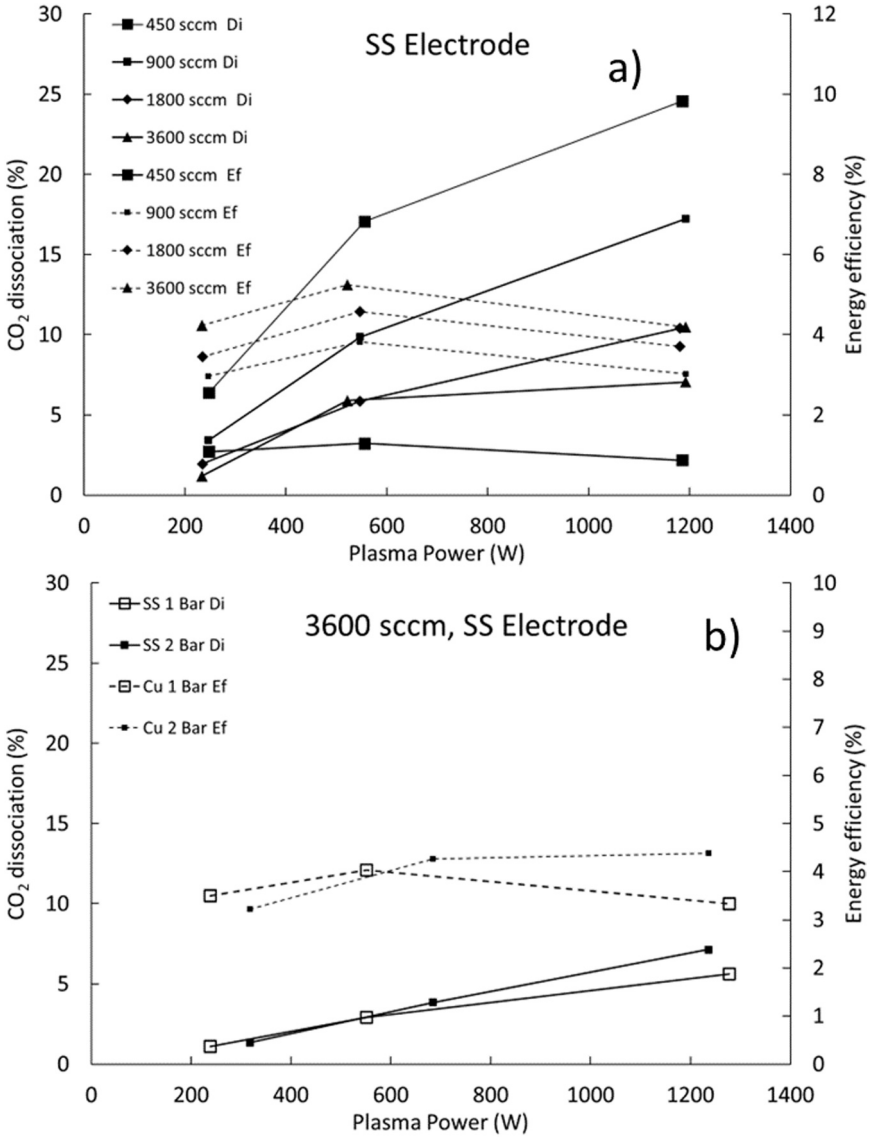

Fig. 3. a) Conversion and energy efficiency with Stainless Steel AISI316 electrode, 1Bar. b) conversion and efficiency for a large 3600sccm flow of CO_2 at 1 and 2 Bar for Copper and SS electrodes.

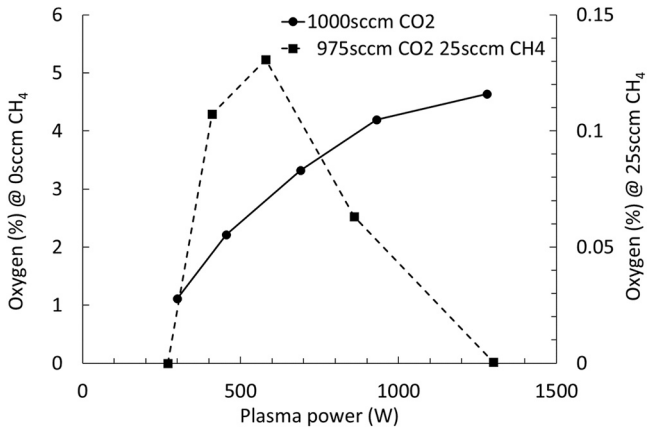

Fig. 4. Oxygen molar fraction in the outstream (solid line) at different plasma power at 1000sccm in pure CO_2 and with 25sccm of CH_4 (dashed line). Water cooled SS electrode.

3.2. Plasma reaction of CO_2 and CH_4

In Table 2 we summarize the conditions explored in the current study, where we have performed two sets of experiments at higher (1000sccm) and lower flow (360sccm) conditions. When using methane, we did not apply copper but only water-cooled SS and aluminium electrodes, and hot uncooled SS.

By adding even small CH_4 amounts the suppression of O_2 in the outstream is observed. In Fig. 4, we show that when adding just 25sccm of CH_4 in a 1000sccm CO_2 flow, oxygen in the outflow can be detected only in small quantities (axis on the right) compared to the oxygen levels of dissociation of pure CO_2 (left axis). Oxygen is not generated at low power (little CO_2 is dissociated) ant it is removed by CH_4 at higher plasma power explaining the bell-shaped curve. In Fig. 4 and Fig. 5, the effect of adding CH_4 is shown when using the cooled SS electrode. (Fig. 6)

The conversion of CO_2 into CO, the dissociation of CH_4 and the production of H_2 are reported in Fig. 5, for plasmas of various power and CH_4 content for two different flow conditions 1000sccm and 360sccm, when using water cooled SS electrodes. At low methane content the

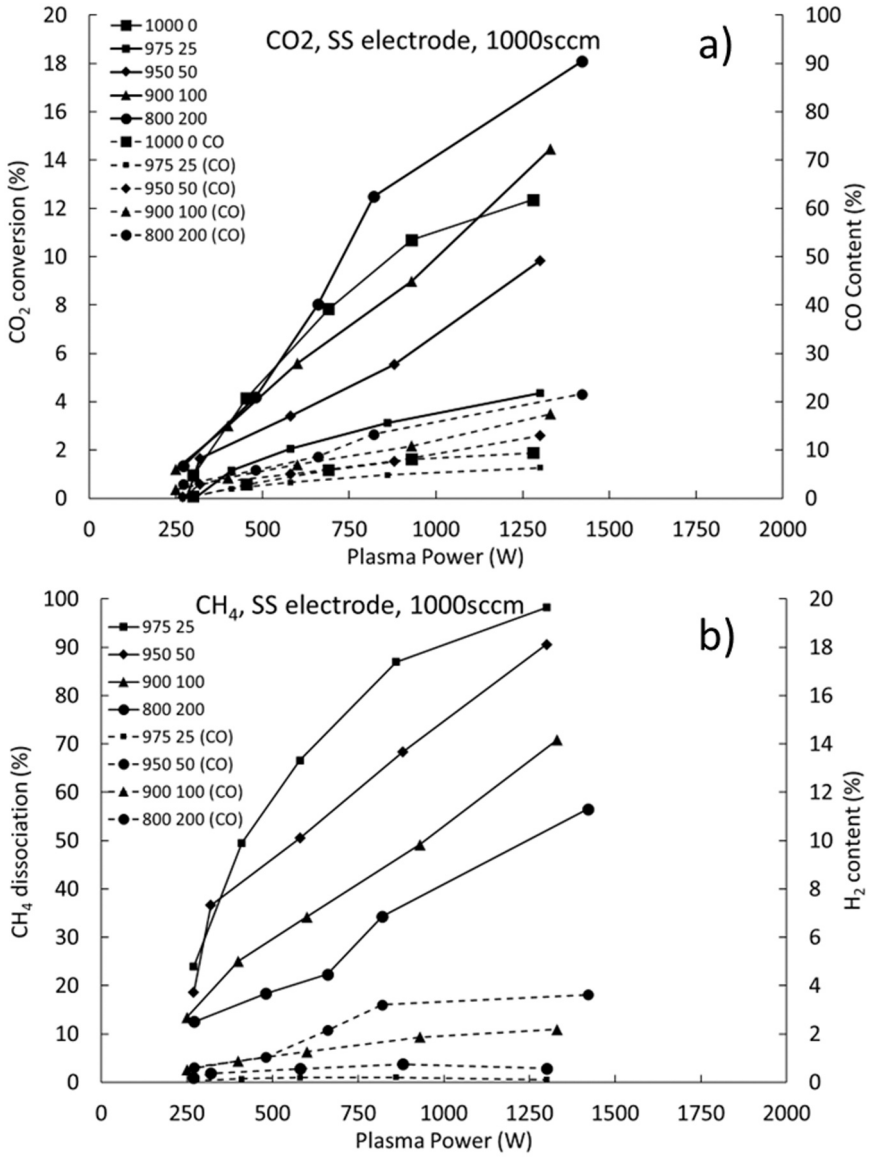

Fig. 5. The effect of different CH_4 flow on the CO_2 conversion and CO molar fraction a) and CH_4 dissociation and H_2 molar fraction b), at 1000sccm. Water cooled SS electrode.

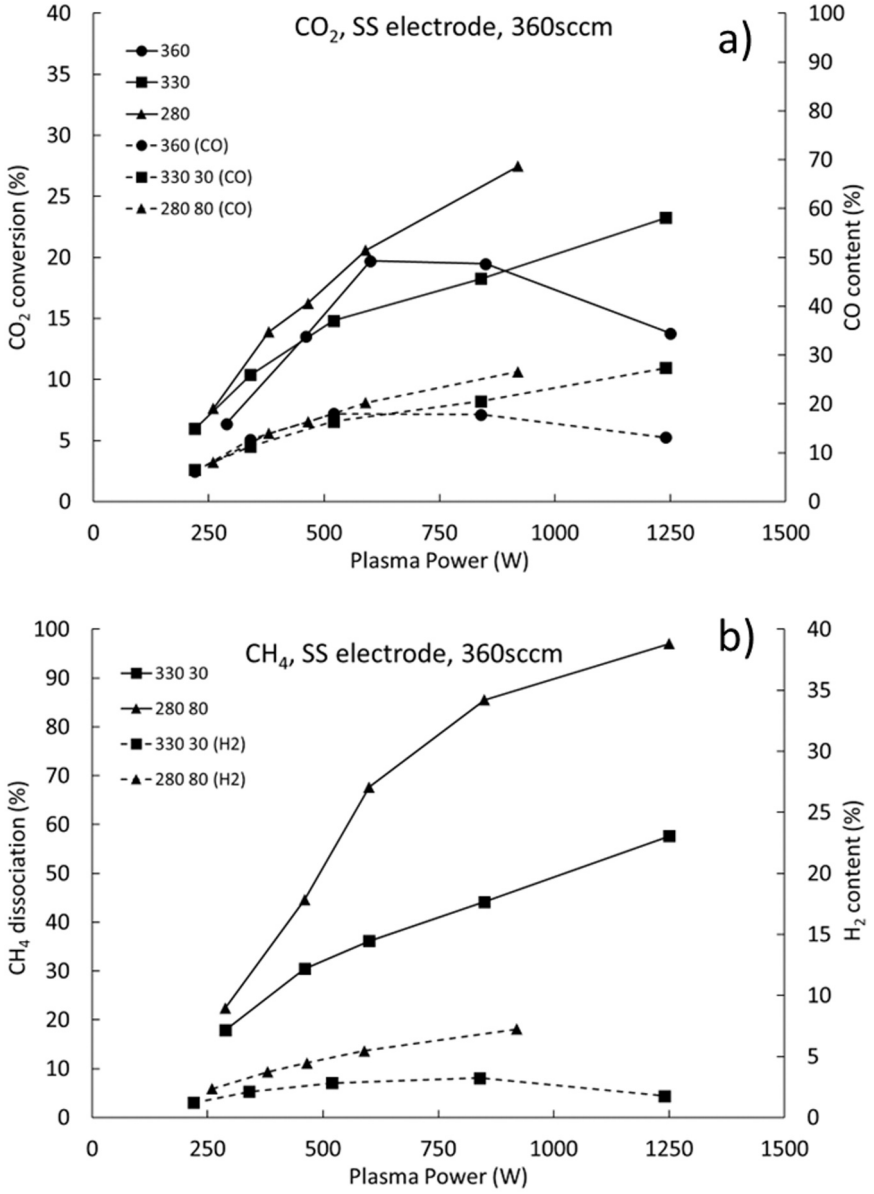

Fig. 6. The effect of different CH_4 flow on the CO_2 conversion and CO molar fraction a), CH_4 dissociation and H_2 molar fraction b), at 360sccm. Water cooled SS electrode.

presence of CH_4 lowers the CO_2 conversion at all power levels, while CH4 dissociation is high. On the other hand, with at 10 % methane content the conversion matches that of pure CO_2, while at 20 % it becomes higher, especially at the higher plasma power side, where the typical saturation behaviour of pure CO_2 plasma dissociation is not observed. The effect is seen in Fig. 5a) for the larger 1000sccm flow, but it is far more evident at 360sccm in Fig. 5b). Here, at high power, dissociation of pure CO_2 not only saturates but decreases at high plasma power, probably due to less optimal plasma parameters and non-linear phenomena. Highest CO_2 conversions are observed to reach 40 % at low flow and high power.

The same picture emerges from figure S5 and figure S6, when we use the water-cooled aluminium electrode instead and applied the same flow and conditions in a different set of experiments. Here the CO_2 conversions is observed to be similar if somehow higher than for the SS electrodes, especially for the larger 1000sccm flow. Currently it is unclear if this is due to better cooling, to a different surface chemistry, including different surface passivation, or to small unaccounted differences in electrode alignment that lead to homogeneities of power deposition in the discharge volume. All considered, large differences did not emerge.

Further we investigated the effect of suppressing the inner electrode cooling for the SS electrode and the results are reported in Fig. 7. In figure S7, we show the measured value of the inner electrode temperature as measured by a thermocouple placed inside the copper electrode support, the surface electrode temperature is expected to be higher than that, of the amounts reported in figure S1c).(Fig. 8)

At higher temperature the conversion of CO_2 and CH_4 dissociation are similar to the water-cooled inner electrode case, with apparently less CO and H_2 being produced at the overall flow of 1000sccm and more at 360sccm, especially for the methane rich conditions with a CO_2 conversion of 45 % and the almost complete CH_4 dissociation.

It is interesting to notice that for the pure CO_2 flow case the CO_2 conversion in this set of experiments (the continuous line with circles) are lower than the values reported in the previous section in Fig. 3, which had been performed earlier on the same system and electrodes. We observe that now the conversion saturates and may decrease when increasing plasma power (most evident in the solid line with circles of

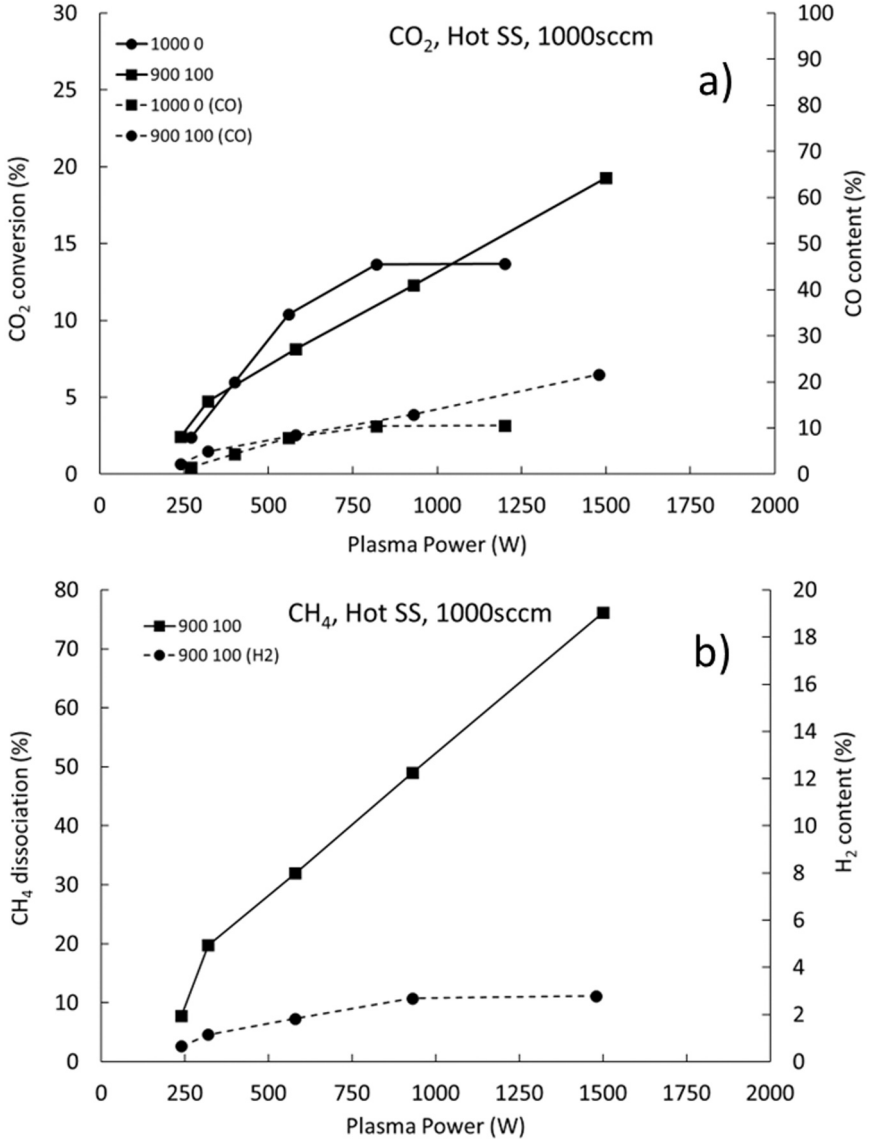

Fig. 7. the conversion of CO_2 and CO molar fraction a), CH_4 dissociation and H_2 molar fraction b), with hot, uncooled SS electrode at 1000sccm. The electrode temperature is in Fig. S7.

Fig. 6a, 7a and 8a) in contradiction with the monotonic increase with power seen in Fig. 3.

Later experiments showed that this effect is due to the presence of surface modifications (and deposits) occurring at the electrode surface, the deposition of (hydrogenated)carbons, that temporarily limit the dissociation reaction in pure CO_2 until the deposit is removed and the electrode surface is recovered to its initial, oxygen passivated surface. To confirm this effect in figure S8 we show a time trace of CO content in the outflow under constant plasma power, that demonstrates the recovery of the conversion of the water-cooled SS electrode. Under pure CO_2 flow and a plasma power of 1200 W, it takes about 30 min of continuous operations for the restoration of the electrode surface. These deposits form during the experimental runs when CH_4 rich, high plasma power conditions are applied and need time to clean off once CH_4 is suppressed from the inlet.

Finally, the effect of working at higher pressure was investigated, by operating the discharge at one selected condition (280 sccm CO_2 + 80 sccm CH_4) at 2 and 3 bar, and results are compared in Fig. 8 with operations at 1 bar.

Overall, the curves are similar, despite the larger residence time in the plasma gap at higher pressure. The different behaviour of the curve at 2 Bar with Al electrode of figure S9 at lower plasma power can be attributed to the imperfect coaxial alignment of the inner electrode, that was corrected for the experiment at 3 bar.

This effect is due to the incomplete and uneven filling by the discharge plasma of the inter-gap volume at lower power. In case of good coaxial alignment, operating at lower power (<700 W) results in a discharge that initially fills the electrode gaps coaxially, often starting from the gas inlet side, but if the alignment is not optimal (consider that the gap is 1 mm only) it may lead to the partial filling of only one discharge sector, a geometry that leaves available through paths for unreacted gas that is not excited by the plasma.

Overall, we conclude that the system can be operated up to 3 Bar pressure without large losses in efficiency, and probably at higher pressure with small modifications to the power supply, mainly to avoid external arching due to the increase of the discharge voltage.

3.3. *Conversion and energy efficiency*

The evaluation of the CO_2 dissociation process efficiency in the presence of methane is not as straightforward as in the case of pure CO_2. For the latter case is easily calculated as the product of the conversion

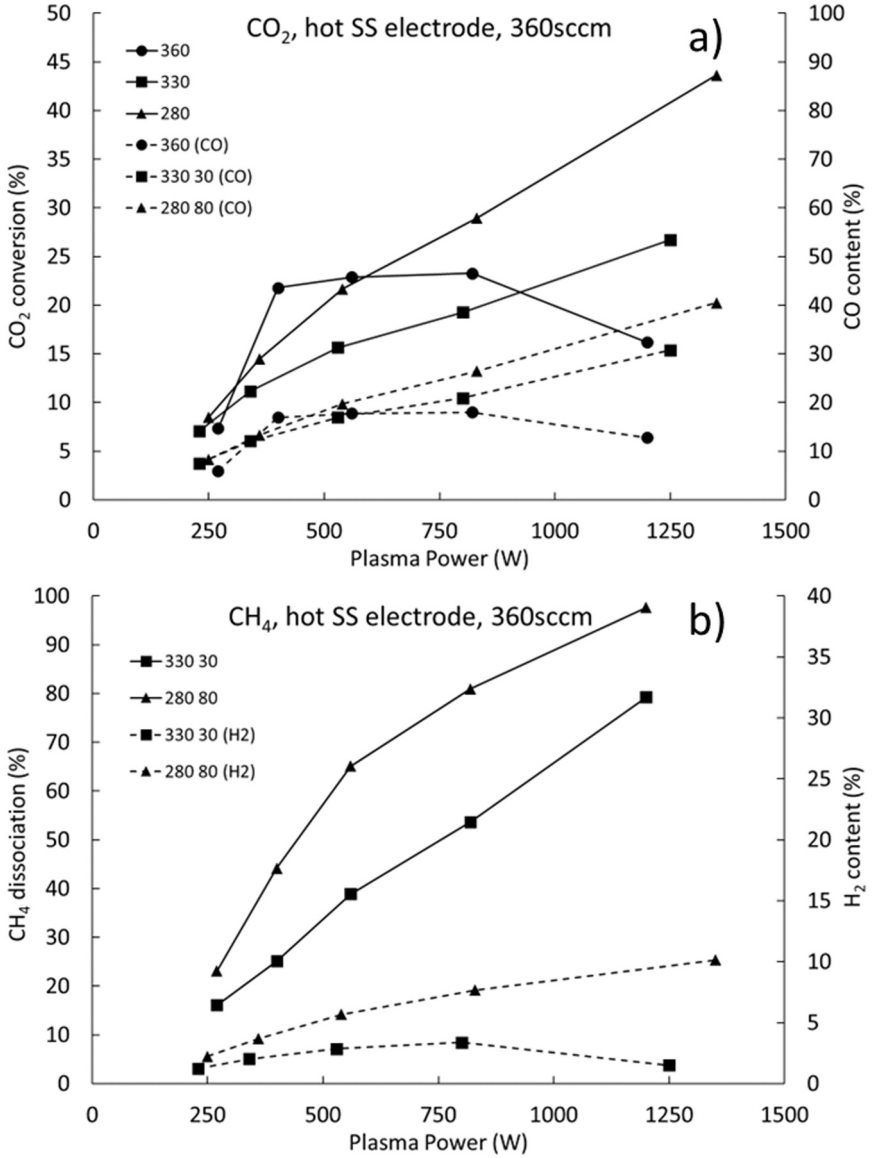

Fig. 8. the conversion of CO_2 and CO molar fraction a), CH_4 dissociation and H_2 molar fraction b), with hot, uncooled SS electrode at 360sccm. The electrode temperature is in Fig. S7.

and the CO_2 flow times the dissociation enthalpy divided by the plasma power.

If the energy efficiency is relevant for the practical application, as in perspective for large scale greenhouse mitigation systems, we may reason as follow. If CH_4 is considered a waste, as in the case of a landfill gas that is either emitted in the atmosphere or flared, its energy content can be neglected, and we can continue to calculate the energy efficiency applying the same formula based on the dissociation enthalpy of CO_2 alone. In other words, if the energy content of CH_4 is not recovered, from the engineering point of view, it is fair to neglect its energy contribution in the energy efficiency calculation.

Therefore, the applied formulas for CO_2 conversion (Eq.5), CH_4 dissociation (Eq.6) and Energy efficiency in the case of pure CO_2 (Eq.7) were:

$$X_{CO_2} = \frac{F_{tot,in} \bullet \gamma_{CO_2,in} - F_{tot,out} \bullet \gamma_{CO_2,out}}{F_{tot,in} \bullet \gamma_{CO_2,in}} \tag{5}$$

$$X_{CH_4} = \frac{F_{tot,in} \bullet \gamma_{CH_4,in} - F_{tot,out} \bullet \gamma_{CH_4,out}}{F_{tot,in} \bullet \gamma_{CH_4,in}} \tag{6}$$

$$\eta_{CO_2}(\%) = \frac{X_{CO_2} \bullet F_{CO_2}}{22.414(\frac{Nl}{mol})} \bullet 60(\frac{s}{\min}) \bullet \frac{\Delta H_{0,diss.}}{P_{plasma}} \tag{7}$$

Where $F_{tot,in}$ and $F_{tot,out}$ are the total molar flow at the inlet and outlet of DBD reactor respectively, $\bullet\gamma_i$ is the molar fraction, $P_{diss.}$ is the theoretical CO_2 dissociation enthalpy, P_{plasma} is the power discharged in the DBD.

Instead, if the CH_4 is regarded as an energy vector, as for the case of a methane fraction of a high-quality biogas that is not scrubbed for the specific purpose, then its energy content that is lost to the grid should be considered. In the latter case the global reaction enthalpy should consider the contribution of CH_4, mainly in the form of the energy released by the formation of all the reaction products.(Fig. 9)

We have calculated the scaling factor between CO_2 conversion and efficiency for the conditions explored in this work and reported for Table 2. The scaling between conversion and energy efficiency is reported in Fig. 10 for the overall flow of 1000sccm and 360sccm. For convenience the values are plotted in a logarithmic scale. Here the continuous, top curve represents the scaling factor for pure CO_2, to be applied if one considers CH_4 as a waste, which obviously leads to a higher "energy efficiency per conversion".

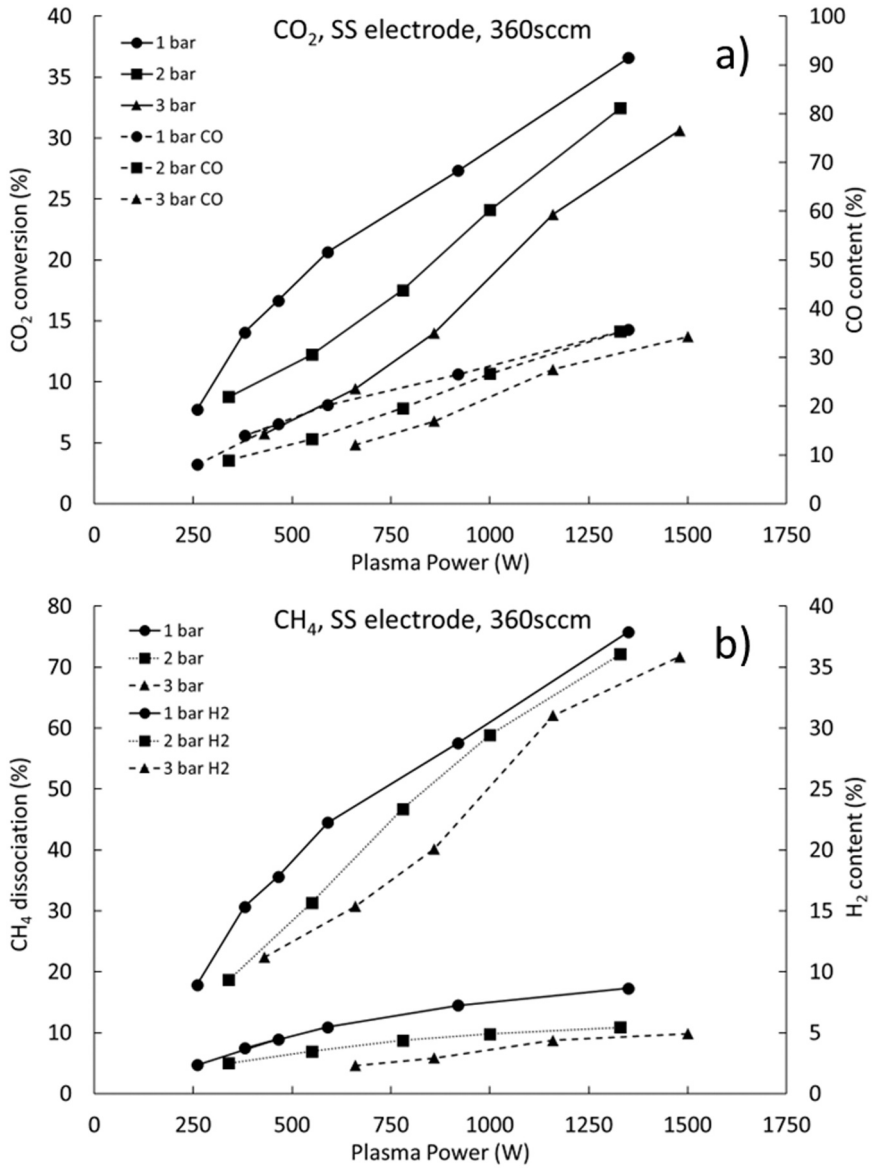

Fig. 9. CO_2 conversion and CO molar fraction a), CH_4 dissociation and H_2 molar fraction b), for respectively 280 and 80 sccm at ambient and high pressure: comparison between 1, 2 and 3 Bar using water cooled SS electrode.

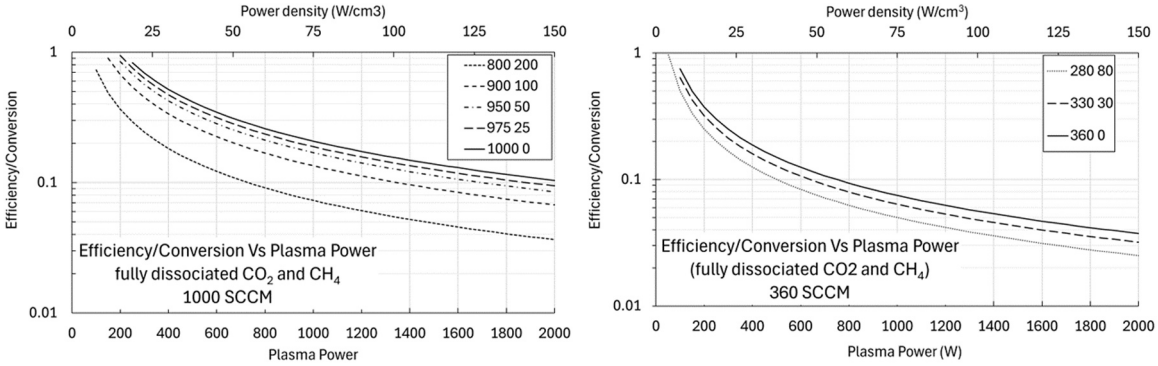

Fig. 10. The adimensional ratio between energy efficiency and conversion, for various gas mixtures and plasma power. In the legend is reported the flow of CO_2 (left) and CH_4 (right).

$$\eta(\%) = \frac{X_{CO_2} \bullet F_{CO_2}}{22.414(\frac{Nl}{mol})} \bullet 60(\frac{s}{\min}) \bullet \frac{\sum_i \Delta H_{f,i} \bullet \dot{n}_i / \dot{n}_{tot}}{P_{plasma}} \quad (8)$$

On a secondary x-axis we have reported the plasma power density (w/cm^3), to supplement information on the SEI (kJ/mol) values reported in Tables 1 and 2.

The curves were calculated based on bond energy differences of the main products, considering full CH_4 and CO_2 dissociation and reaction. The continuous line was applied for the calculation of the energy efficiency in Fig. 3, for the pure CO_2 case.

3.4. Optical emission spectroscopy

Some insight on the reactions occurring inside the discharge plasma was provided by optical emission spectra collected during the operations. The spectra were measured through the water, cooling the outer mesh electrode and dielectric, and the double quartz reaction wall as in Fig. 2.

The spectrometer does not have a sufficient resolution to provide quantitative evaluations of the plasma temperature and of the rotational gas temperature [36] neither was it possible to apply the line ratio method for the Ar atomic lines [37] since the method only works at low pressure. However, it is possible determine the changes in the main excited species in the different discharge conditions, that gives some clues on the plasma chemistry, complementary to the downstream observations carried by mass spectroscopy.

The spectra were analysed, and the lines identified using the "Spectrum Analyzer" software package [38]. At high plasma power (2 kW), the situation is exemplified in figure S10 to S13. Different spectral regions are dominated by different band systems from ionized atoms and molecules. At shorter wavelength the C I atomic line at 297 nm, the CH I lines at 314 nm and 431 nm, then the band system of CO_2 I lines between 300 and 400 nm, at intermediate wavelengths the emission from CO (mainly the Angstrom system) between 400 and 700 nm, then the Ar I lines around 700 nm and the oxygen O I line at 777 nm. In figure S10 the spectrum of a pure CO_2 plasma shows a strong CO_2 I and CO I emission, and strong emission from O I. The O I emission is almost fully quenched by the addition of a small quantity of CH_4 in

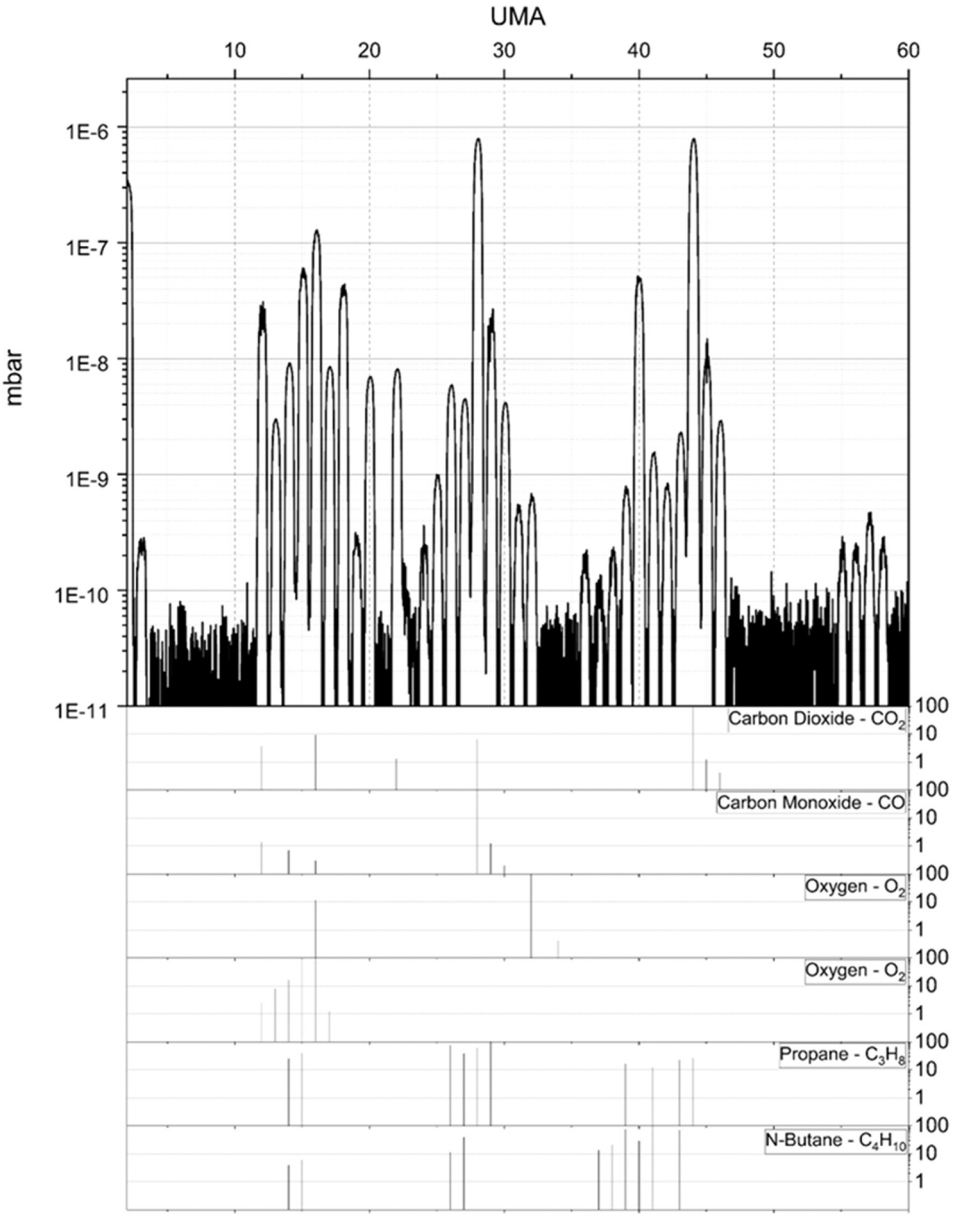

Fig. 11. The full spectrum of fragments during CH4 CO2 operations.

figure S11: just 25 SCCM reduces the emission from CO I and already fully suppress the O I emission at 777 nm, in line with what is observed respectively in Fig. 6a (reduced CO conversion) and in Fig. 4 (no O_2 outflow).

Figures S12 and S13 apply instead to the 800 CO_2 200 CH_4 case. Fig. 11 is collected in the middle of the discharge and shows that with higher methane content we have very strong CO emission (high conversion as in Fig. 5a), the CH I 431 nm band appears and the C_2 Swan bands also intensify indicating the formation of C_2 and higher carbon compounds [17]. Here, stronger CH I line emission at 314 nm and 431 nm is evident together with lower CO and higher CO_2, and corresponds to the visual observation of a discharge section that exhibits a different colour at the inlet. Instead, if we point the OSE collecting lens towards the top of the discharge where the gas inlet is, the spectrum changes as reported in figure S13.

It is interesting to notice that as soon as CH_4 is added to the plasma the O I lines is strongly reduced to almost naught, confirming that the two plasma reactions, (2) and (4), are strongly coupled and oxygen is readily scavenged by methane and its fragments ad soon as it is produced, correspondingly such small methane flow inhibits the CO_2 dissociation as seen in Figs. 5a and 6a.

As seen also in Figs. 4 and 5 the presence of the smallest amount of CH4 suppresses oxygen but it also strongly inhibits the process of dissociation itself, wither this is due to the formation of H that cools the vibrational excitation of CO_2 or to the formation of OH that reacts with CO it is not clear. As discussed in the introduction it was found that adding small amounts of H_2 and He to CO_2 gas mixtures inhibited the dissociation and was in the past functional to increase the laser efficiency.

3.5. *Water, hydrocarbons, and carbon formation*

The formation of water was documented by copious condensation at the bottom of the reactor, on the surface of the inner cooled electrode and on the inner quartz wall as seen at the bottom of figure S14a). Although we did measure water vapor with the mass spectrometer, we found that measurement unreliable in the actual experimental set-up, since the vapour content in the outstream heavily depends on the temperature, pressure, of all reactor parts and on flow.

The formation of larger molecules and hydrocarbon was investigated by performing full mass scan at selected plasma conditions. We present here the more methane rich conditions CO_2 800 sccm and CH_4 200 sccm with cooled SS electrodes.

As reference the data for 1000 sccm of CO_2 (for comparison with experiments with CH_4 a 2 %v/v of Ar was added) are presented in figure S15 with 750 W power. Beyond Ar, the mass spectrometer fragmentation evidences the presence of CO_2, CO and O_2. The fragments in experiments with CH_4 with a water cooled steel electrode, are reported in Fig. 11 (800 CO_2, 200 CH_4, 20 Ar with 1200 W as in Fig. 5) and highlight the presence of higher hydrocarbons up to C3 and C4 and relative oxides/alcohols, in line with previous reports [17]. The scan was performed after reaching stationary conditions during plasma operations. The overall measured quantities of these compounds in Fig. 11 in the in the actual experimental conditions do not alter the main reaction energetic, but should be considered in developing the reactor technology.

After tests performed at 3 Bar and at high power (>1 kW) with cooled aluminium electrodes we found that some dark deposits had formed on the electrode surface, as seen in figure S14b).

The position on the electrodes of the solid deposits were consistent with the location of random hot spots that were observed on the electrode surface during the operation of the discharge, that showed an optical emission spectrum typical of thermal emission (red and IR continuum, not reported here). We attribute these deposits to CO disproportionation driven by pressure and high CO concentration on hot spots.

One may speculate that operating at higher pressure it may be possible to investigate if some form of plasma driven solid carbon sequestration [24] with water condensation from CH_4 and CO_2 may deserve some further investigation for practical application.

4. Conclusions

In conclusion in this work, we have investigated the dissociation of CO_2 into CO and O_2 using pure CO_2 as a feed gas, applying different electrode materials, pressures, flow, and plasma power. The tests were performed in a water cooled DBD system that is capable to operate with up to 2 kW of plasma power. The results are overall comparable to previous research literature data, that confirm the well-known trade-off between conversion and energy efficiency. It confirms that the DBD plasma system does not have the correct electric field and electron density for energy efficient CO_2 dissociation.

Furthermore, we have investigated the effect of adding small quantities of CH_4, (up to 1/3.5 of the CO_2 flow) to the CO_2 inlet in order to take two possible advantages: the first is the possibility to apply the system to the fully electric valorisation of waste or landfill greenhouse gases that are actually flared, the second being the suppression of O_2 from the dissociated flow and the production of H_2. Removing O_2 is vital for the use of a main CO output, for example for its downstream conversion in H_2 by WGS.

At the same time, adding very small amounts of CH_4 completely removed oxygen form the products, but also negatively influenced the dissociation process. The results show that when high plasma power is applied to the CO_2 CH_4 mixture high dissociation is achieved for CH_4 and high conversion for CO_2 into CO, and that the presence of CH_4 effectively scavenges for the oxygen released by the dissociation.

We believe that the same will apply when better, CO_2 plasma dissociation systems will be found more energy efficient than the actual DBDs, providing a viable approach to the valorisation and management of greenhouse wastes. We also remark that high power plasma, devoid of catalysts can contribute to remove and destroy a wide spectrum of pollutants, being mostly insensitive to their presence, providing strongly oxidising environment when applied to CO_2, that tuning the flow to CH_4 becomes reducing.

Finally, we have observed the formation of higher hydrocarbons and graphitic deposits when the system is operated.

CRediT authorship contribution statement

Nicola Lisi: Writing – review & editing, Writing – original draft, Visualization, Validation, Project administration, Methodology, Investigation, Funding acquisition, Formal analysis, Data curation, Conceptualization. **Umberto Pasqual Laverdura:** Writing – review & editing, Writing – original draft, Visualization, Methodology, Investigation, Funding acquisition, Formal analysis, Data curation, Conceptualization.

Declaration of Competing Interest

The authors declare that they have no known competing financial interests or personal relationships that could have appeared to influence the work reported in this paper.

Data availability

Data will be made available on request.

Acknowledgements

The research was carried out with the support from the European Union's Horizon 2020 research and innovation programme under grant agreement No. 101006656, from the Electric System Research Programme, Project 1.6, WP 4, by the Ministry for the Environment and Energy Security and by the European Union – NextGeneration EU under PNRR Piano Operativo della Ricerca Idrogeno "POR H2", WP1,

LA1.1.21.

Appendix A. Supporting information

Supplementary data associated with this article can be found in the online version at doi:10.1016/j.jcou.2024.102931.

References

[1] U. Kogelschatz, B. Eliasson, W. Egli, U. Kogelschatz, B. Eliasson, W.E.D. D. Principle, Dielectric-barrier discharges. principle and applications, J. De. Phys. Iv (1997), https://doi.org/10.1051/jp4:1997405ff.ffjpa-00255561.

[2] I.G. Belousov, V.A. Legasov, and V.D. Rusanov, A plasmochemical concept for thermochemical hydrogen production, vol. 5, no. 1, pp. 1–6, 1980.

[3] A. Fridman, Plasma Chemistry, Cambridge University Press, 2008.

[4] W. Bongers, et al., Plasma-driven dissociation of CO2 for fuel synthesis, Plasma Process. Polym. vol. 14 (6) (2017), https://doi.org/10.1002/ppap.201600126.

[5] R. Snoeckx, A. Bogaerts, Plasma technology-a novel solution for CO2 conversion? R. Soc. Chem. (2017) https://doi.org/10.1039/c6cs00066e.

[6] S. Li, G.De Felice, S. Eichkorn, T. Shao, F. Gallucci, A review on plasma-based CO2 utilization: process considerations in the development of sustainable chemical production, Plasma Sci. Technol. (2024), https://doi.org/10.1088/2058-6272/AD52C4.

[7] M. Ramakers, I. Michielsen, R. Aerts, V. Meynen, A. Bogaerts, Effect of argon or helium on the CO2 conversion in a dielectric barrier discharge, Plasma Process. Polym. vol. 12 (8) (2015) 755–763, https://doi.org/10.1002/ppap.201400213.

[8] M. Songolzadeh, M. Soleimani, M.T. Ravanchi, R. Songolzadeh, W. Han, and V.A. Rogov, Carbon Dioxide Separation from Flue Gases: A Technological Review Emphasizing Reduction in Greenhouse Gas Emissions, 2014, doi: 10.1155/2014/828131.

[9] S. Nanda, F. Berruti, Municipal solid waste management and landfilling technologies: a review, Environ. Chem. Lett. vol. 19 (2) (2021) 1433–1456, https://doi.org/10.1007/S10311-020-01100-Y/FIGURES/9.

[10] V.A. Legasov *et al.*, Nonequilibrium plasmochemical process of the CO 2 decomposition in HF and SHF discharges, 1978. [Online]. Available: ⟨http://www.mathnet.ru/eng/agreement⟩.

[11] S.R. Snoeckx, A. Bogaerts, R. Snoeckx, Plasma technology-a novel solution for CO 2 conversion? As featured in: plasma technology-a novel solution for CO 2 conversion? Chem. Soc. Rev. vol. 46 (2017) 5805, https://doi.org/10.1039/c6cs00066e.

[12] N. Lisi, U. Pasqual Laverdura, R. Chierchia, I. Luisetto, S. Stendardo, A water cooled, high power, dielectric barrier discharge reactor for CO2 plasma dissociation and valorization studies, Sci. Rep. vol. 13 (1) (2023), https://doi.org/10.1038/s41598-023-33241-9.

[13] D. Zhang *et al.*, Tuning of Conversion and Optical Emission by Electron Temperature in Inductively Coupled CO 2 Plasma, 2018, doi: 10.1021/acs.jpcc.8b04716.

[14] G. Chen, et al., A novel plasma-assisted hollow fiber membrane concept for efficiently separating oxygen from CO in a CO2 plasma, Chem. Eng. J. vol. 392 (2020), https://doi.org/10.1016/j.cej.2019.123699.

[15] N. Nauels, S. Herzog, M. Modigell, C. Broeckmann, Membrane module for pilot scale oxygen production, J. Memb. Sci. vol. 574 (2019) 252–261, https://doi.org/10.1016/j.memsci.2018.12.061.

[16] M. Kraus, B. Eliasson, U. Kogelschatz, A. Wokaun, CO2 reforming of methane by the combination of dielectric-barrier discharges and catalysis (in), Phys. Chem. Chem. Phys. (2001) 294–300, https://doi.org/10.1039/b007015g.

[17] B. Eliasson, C.J. Liu, U. Kogelschatz, Direct conversion of methane and carbon dioxide to higher hydrocarbons using catalytic dielectric-barrier discharges with zeolites, Ind. Eng. Chem. Res vol. 39 (5) (2000) 1221–1227, https://doi.org/10.1021/ie990804r.

[18] S.M. Chun, Y.C. Hong, D.H. Choi, Reforming of methane to syngas in a microwave plasma torch at atmospheric pressure, J. CO2 Util. vol. 19 (2017) 221–229, https://doi.org/10.1016/j.jcou.2017.03.016.

[19] M. Dors, T. Izdebski, A. Berendt, J. Miceraczyk, Hydrogen production via biomethane reforming in DBD reactor, Accessed: Mar. 07, 2024. [Online]. Available: Int. J. Plasma Environ. Sci. Technol. no. 6 (2012) 93–97, https://doi.org/10.34343/ijpest.2012.06.02.093.

[20] B. Sarmiento, J.J. Brey, I.G. Viera, A.R. González-Elipe, J. Cotrino, V.J. Rico, Hydrogen production by reforming of hydrocarbons and alcohols in a dielectric barrier discharge, J. Power Sources vol. 169 (1) (2007) 140–143, https://doi.org/10.1016/j.jpowsour.2007.01.059.

[21] A. Ozkan, T. Dufour, G. Arnoult, P. De Keyzer, A. Bogaerts, F. Reniers, CO2-CH4 conversion and syngas formation at atmospheric pressure using a multi-electrode dielectric barrier discharge, J. CO2 Util. vol. 9 (2015) 74–81, https://doi.org/10.1016/j.jcou.2015.01.002.

[22] O. Akande, B.J. Lee, Plasma steam methane reforming (PSMR) using a microwave torch for commercial-scale distributed hydrogen production, Int. J. Hydrog. Energy vol. 47 (5) (2022) 2874–2884, https://doi.org/10.1016/j.ijhydene.2021.10.258.

[23] S. Müller, E. Ströfer, M. Kohns, K. Münnemann, E. von Harbou, H. Hasse, Investigation of partial oxidation of methane in a cold plasma reactor with detailed product analysis, Plasma Chem. Plasma Process. vol. 43 (2) (2023) 513–532, https://doi.org/10.1007/s11090-022-10308-5.

[24] Z. Li, et al., Boudouard reaction driven by thermal plasma for efficient CO2 conversion and energy storage, J. Energy Chem. vol. 45 (2020) 128–134, https://doi.org/10.1016/j.jechem.2019.10.007.

[25] V. Palma, D. Pisano, M. Martino, P. Ciambelli, Structured catalysts with high thermoconductive properties for the intensification of Water Gas Shift process, Chem. Eng. J. vol. 304 (2016) 544–551, https://doi.org/10.1016/J.CEJ.2016.06.117.

[26] A.K. Grebenko, et al., High-quality graphene using boudouard reaction, Adv. Sci. vol. 9 (12) (2022), https://doi.org/10.1002/advs.202200217.

[27] The effect of water vapour and hydrogen on the gas composition of a sealed-off CO2 laser.

[28] A.L.S. Smith, T.H. Bett, P.G. Browne, The effects of gas additives on TEA CO2 lasers, IEEE J. Quantum Electron vol. 11 (7) (1975) 335–340, https://doi.org/10.1109/JQE.1975.1068640.

[29] T.F. Deutsch, Effect of hydrogen on CO2 TEA lasers, Appl. Phys. Lett. vol. 20 (8) (1972) 315–316, https://doi.org/10.1063/1.1654164.

[30] R. Torabi, K. Silakhori, and H. Salmani, cite this article: Yutaka Uchida et al, 1990.

[31] V.D. Rusanov, A.A. Fridman, and G.V. Sholin, The physics of a chemically active plasma with nonequilibrium vibrational excitation of molecules, 1981.

[32] C. Douat, et al., The role of the number of filaments in the dissociation of CO2 in dielectric barrier discharges, Plasma Sources Sci. Technol. vol. 32 (5) (2023), https://doi.org/10.1088/1361-6595/acceca.

[33] S. Bollanti, P. Di Lazzaro, F. Flora, T. Letardi, N. Lisi, C.E. Zheng, Space and time resolved discharge evolution of a large volume X-ray triggered XeCl laser system, Appl. Phys. B Photo Laser Chem. vol. 55 (1) (1992), https://doi.org/10.1007/BF00348619.

[34] N. Lisi, U.P. Laverdura, R. Chierchia, I. Luisetto, and S. Stendardo, A water cooled, high power, dielectric barrier discharge reactor for CO 2 plasma dissociation and valorization studies, 123AD, doi:10.1038/s41598-023-33241-9.

[35] M. Hołub, On the measurement of plasma power in atmospheric pressure DBD plasma reactors (in), Int. J. Appl. Electromagn. Mech. (2012) 81–87, https://doi.org/10.3233/JAE-2012-1446.

[36] Y. Du, K. Tamura, S. Moore, Z. Peng, T. Nozaki, P.J. Bruggeman, CO(B 1Σ+→A 1Π) Angstrom system for gas temperature measurements in CO2 containing plasmas, Plasma Chem. Plasma Process. vol. 37 (1) (2017) 29–41, https://doi.org/10.1007/s11090-016-9759-5.

[37] X.M. Zhu, Y.K. Pu, Optical emission spectroscopy in low-temperature plasmas containing argon and nitrogen: determination of the electron temperature and density by the line-ratio method, J. Phys. D. Appl. Phys. vol. 43 (40) (2010), https://doi.org/10.1088/0022-3727/43/40/403001.

[38] Z. Navrátil, D. Trunec, R. Šmíd, L. Lazar, A software for optical emission spectroscopy-problem formulation and application to plasma diagnostics, Czechoslov. J. Phys. vol. 56 (SUPPL. 2) (2006) B944–B951, https://doi.org/10.1007/S10582-006-0308-Y/METRICS.